



ISSN 0975-413X  
CODEN (USA): PCHHAX

Der Pharma Chemica, 2017, 9(2):90-98  
(<http://www.derpharmachemica.com/archive.html>)

## Synthesis, Characterization, DNA binding, DNA Cleavage and Antibacterial Studies of Ni(II) and Cu(II) Complexes of Pyridoxal Semicarbazone

Saritha Aduri<sup>1</sup>, Venkata Ramana Reddy CH<sup>2</sup>, Sireesha B<sup>1\*</sup>

<sup>1</sup>Department of Chemistry, Nizam College, Osmania University, Hyderabad-500001, India

<sup>2</sup>Department of Chemistry, Jawaharlal Nehru Technological University, Hyderabad-500085, India

### ABSTRACT

*Ni(II) and Cu(II) complexes of Pyridoxal Semicarbazone (PLSC) have been synthesized and characterized by elemental analyses, molar conductance and magnetic susceptibility measurements, thermal analysis, ESI-MS, IR and electronic spectral studies. DNA-binding properties of these metal complexes with CT-DNA in a potassium phosphate buffer (pH 7.2) were investigated using UV-Vis absorption spectroscopy, fluorescence spectroscopy and viscosity measurements. Experimental studies suggest good DNA binding ability of these metal complexes through intercalation. The cleavage of plasmid pBR322 DNA without any additives was monitored by gel electrophoresis and these complexes exhibited hydrolytic cleavage of plasmid DNA. The in vitro antibacterial activity of the synthesized complexes has been tested against gram positive and gram negative bacteria.*

**Keywords:** Antibacterial activity, DNA binding, Cleavage activity, Metal complexes, Pyridoxal semicarbazone

### INTRODUCTION

Transition metal complexes of Schiff base ligands based on semicarbazone and thiosemicarbazone have made a major contribution in the development of coordination chemistry [1]. Their study attracted due attention because of their ease of formation, structural diversity, multidentate nature and biological applications [2]. Numerous structural and biological studies have been made on the metal complexes of semicarbazones [3]. Ni(II) complexes of semicarbazone ligand show anticancer activity [4], antibacterial and antifungal activities [5] and Cu(II) complexes containing semicarbazone displayed antifungal [6], antioxidant, radical scavenging and antibacterial activities [7]. Pyridoxal Semicarbazone (PLSC), a Schiff base derived from pyridoxal (a form of vitamin B<sub>6</sub>) and its transition metal complexes are investigated by many researchers [8,9]. Several reports have been made on the synthesis, structure and the biological activity of transition metal complexes incorporating PLSC ligand. In its metal complexes PLSC can exist as neutral, mono and dianionic forms [10]. It is reported as tridentate ONO ligand, which coordinates through hydrazine nitrogen, phenolic and carbonyl oxygen atoms and an excellent chelating agent [11]. Its metal complexes exhibit enormous potential as biologically active agents. Transition metal complexes of PLSC show antimicrobial activity [12], anticancer activity [13] and cytotoxicity [14]. However, no significant studies were made on the DNA binding and cleavage properties of metal complexes of PLSC.

DNA binding properties of transition metal complexes have been extensively studied during the past two decades as they can be used as anticancer drugs and DNA structural probes [15]. Metal complexes interact with the double helix DNA in either covalent or non-covalent way. The non-covalent way includes three modes of binding, i.e., electrostatic effects, groove binding and intercalation, among which intercalation is the most important binding mode [16]. Small molecules when bind to DNA through intercalation, can damage DNA in cancer cells and hence can be used as anticancer drugs [17]. The ability of transition metal complexes to cleave nucleic acids efficiently with a high level of selectivity for a site or sequence offers many applications for the manipulation of genes and development of novel therapeutics [18].

The aim of the present work is to synthesize the Ni(II) and Cu(II) complexes of pyridoxal semicarbazone, to understand their structure and to evaluate their DNA binding and cleavage properties along with antibacterial activity.

## EXPERIMENTAL

**Materials and reagents**

All the chemicals were procured from Sigma Aldrich and of analytical grade and used without further purification. Ligand was synthesized according to a reported procedure [19].

**Methods***Instrumentation*

Elemental analyses (% CHN) were obtained using Thermo Finnigan 1112 elemental analyzer. ESI mass spectra of the complexes were recorded on LCMS 2010A, Shimadzu spectrometer. FT-IR spectra of the complexes were recorded using KBr pellets in the range of 4000-250  $\text{cm}^{-1}$  on a Shimadzu IR Prestige-21 FTIR spectrophotometer. UV-Vis spectra in DMSO solution were recorded on Systronics UV-Vis Double beam spectrophotometer 2201 in the range of 200-1000 nm. The molar conductivity was measured with a Digisun digital conductivity bridge using a freshly prepared solution of the complexes in DMSO. Thermogravimetric (TG) analyses were performed using Shimadzu TGA-50H in nitrogen atmosphere in the temperature range of 0°C to 1000°C with a heating rate of 20°C per min. Magnetic susceptibilities were measured at room temperature on Faraday balance model 7550 using  $\text{Hg}[\text{Co}(\text{NCS})_4]$  as the internal standard. Diamagnetic corrections were made by using Pascal's constants [20]. DNA cleavage experiments were performed with the help of Biotech electrophoresis system supported by Genei power supply over a potential range of 50-500 V, visualized and photographed by Biotech Transilluminator system.

*DNA binding activity by electronic absorption spectra*

The binding of complexes with CT DNA was measured in potassium phosphate buffer solution (pH 7.2). A solution of DNA in the buffer gave a ratio of UV absorbance at 260 nm and 280 nm,  $A_{260}/A_{280}$  of 1.85-1.9, indicating that the DNA was sufficiently free of protein. The concentration of DNA was determined from the UV absorbance at 260 nm using the extinction coefficient  $\epsilon_{260} = 6600 \text{ M}^{-1} \text{ cm}^{-1}$ . The absorbance titrations were performed at a fixed concentration of complexes and varying the concentration of double stranded CT-DNA (2-20  $\mu\text{M}$ ). While measuring the absorption spectra, a proper amount of CT-DNA was added to both compound solution and the reference solution to eliminate the absorbance of CT DNA itself. Concentrated stock solutions of the complexes were prepared by dissolving the complexes in DMSO and diluting suitably with the corresponding buffer to the required concentration (20  $\mu\text{M}$ ) for all the experiments. After the addition of DNA to the metal complex, the resulting solution was allowed to equilibrate for 10 min, after which absorption readings were noted. The data were then fit to the following equation to obtain intrinsic binding constant  $K_b$ .

$$[\text{DNA}]/[\epsilon_a - \epsilon_f] = [\text{DNA}]/[\epsilon_b - \epsilon_f] + 1/K_b[\epsilon_b - \epsilon_f] \quad (1)$$

Where [DNA] is the concentration of DNA in base pairs,  $\epsilon_a$  is the extinction coefficient observed for the absorption band at the given DNA concentration,  $\epsilon_f$  is the extinction coefficient of the complex free in solution, and  $\epsilon_b$  is the extinction coefficient of the complex when fully bound to DNA. A plot of  $[\text{DNA}]/[\epsilon_a - \epsilon_f]$  versus [DNA] gave a slope  $1/[\epsilon_b - \epsilon_f]$  and Y intercept equal to  $(1/K_b)[\epsilon_b - \epsilon_f]$ , respectively. The intrinsic binding constant  $K_b$  is the ratio of the slope to the intercept [21].

*Competitive DNA binding fluorescence experiments*

Relative binding of the complexes to CT DNA was studied using fluorescence spectroscopy, by the displacement of ethidium bromide (EB) bound to CT DNA in a potassium phosphate buffer solution (pH 7.2) [22]. In a typical experiment, 480  $\mu\text{l}$  of CT DNA (20  $\mu\text{M}$ ) solution was added to 2020  $\mu\text{l}$  of EB in buffer solution  $\{[\text{DNA}]/[\text{EB}]=1\}$ . The fluorescence intensity was measured upon excitation at  $\lambda_{\text{max}} = 520 \text{ nm}$ ; maximum emission was observed at  $\lambda_{\text{max}} = 605 \text{ nm}$ . The changes in fluorescence intensities at 605 nm of EB bound to DNA were recorded with an increasing amount of the complex concentration (from its 50  $\mu\text{M}$  stock solution). Stern-Volmer quenching constants were calculated using the equation  $I_0/I = 1 + K_{sv}r$ , where  $I_0$  and  $I$  are the fluorescence intensities in the absence and presence of the complex respectively,  $K_{sv}$  is a linear Stern-Volmer quenching constant and  $r$  is the ratio of total concentration of complex to that of DNA. The value of  $K_{sv}$  is given by the ratio of slope to intercept in a plot of  $I_0/I$  Vs [complex]/[DNA].

*Viscosity measurements*

Viscosity measurements were carried out with the Ostwald viscometer, maintained at 25°C in a thermostatic water bath. Each complex (50  $\mu\text{M}$ ) was introduced into CT-DNA solution (300  $\mu\text{M}$ ) in phosphate buffer (pH 7.2) present in the viscometer. Flow time of solutions was recorded in triplicate for each sample and an average flow time was calculated. Data were presented as  $(\eta'_{sp}/\eta_{sp})^{1/3}$  versus the ratio of the concentration of the complex to CT-DNA, where  $\eta'_{sp}$  is the viscosity of CT-DNA in the presence of the complex and  $\eta_{sp}$  is the viscosity of CT-DNA alone [23].

*DNA cleavage studies*

Agarose gel electrophoresis technique was used to monitor the DNA cleavage ability of the metal complexes on super coiled pBR 322 DNA. Generally, plasmid DNA is converted from super coiled DNA (Form I) to nicked circular (Form II) and linear forms (Form III) [24]. In the experiment, plasmid DNA (300 ng/3  $\mu\text{l}$ ) was treated with the complexes in DMSO (20-60  $\mu\text{M}$ ) in 5 mM Tris. HCl/50 mM NaCl buffer (pH 7.2). The mixture was incubated for 1 h at 37°C. A loading buffer containing 1% bromophenol blue and 40% Sucrose (1  $\mu\text{l}$ ) was added and loaded onto a 0.8% agarose gel containing EB (1  $\mu\text{g/ml}$ ). The gel was run in TAE buffer (40

mM Tris base, 20 mM Acetic acid, 1 mM EDTA, pH 8.3) at a constant voltage 60 V for 2 h until the bromophenol blue had traveled through 75% of the gel. The bands were visualized by viewing the gel on a transilluminator and photographed.

#### Antibacterial activity

The complexes are screened for their antibacterial activity using agar well diffusion method against two gram positive bacteria such as *Staphylococcus aureus* and *Bacillus subtilis* and two gram negative bacteria such as *Escherichia coli* and *Pseudomonas aeruginosa* at a concentration of 1000  $\mu\text{g/mL}$  [25].

### SYNTHESIS OF METAL COMPLEXES

#### Synthesis of Ni(II)-PLSC

Ni(II)-PLSC was prepared by the addition of 0.228 g (1 mmol)  $\text{NiCl}_2 \cdot 6\text{H}_2\text{O}$  (in 10 ml distilled water) to a hot aqueous solution 0.5 g (2 mmol) of the Schiff base ligand (40 ml distilled water) and refluxed for 2 h. A red colored precipitate was formed on adjusting the pH to 7 using a mixture of methanol and ammonia solution. The mixture was continued to reflux for another hr. Then the precipitate was filtered, washed several times with hot distilled water, finally with petroleum ether and air dried.

#### [Ni(HL $\cdot$ ).Cl.2H $_2$ O]

(Yield: 0.29 g, 68%). IR:  $\nu_{\text{max}}/\text{cm}^{-1}$ : 3437 s, 3331 m, 2873 m, 1577 m, 1558 m, 1500 m, 1259 m, 1145 m, 520-550 m (Ni-O), 450-470 m (Ni-N), 310-350 (Ni-Cl). ESI-MS in MeOH: m/z 355 [ $\text{M}^+\text{H}$ ]. Elemental analysis: Found (calc.) for  $\text{C}_9\text{H}_{15}\text{NiN}_4\text{O}_5\text{Cl}$ : C, 32.03 (32.23); H, 4.73 (4.77); N, 16.70 (16.71) %.  $\mu_{\text{eff}}=2.8835$  B.M.  $\Lambda_{\text{M}}[\Omega^{-1}\text{cm}^2\text{M}^{-1}, 10^{-3}, \text{DMSO}]$ : 005

#### Synthesis of Cu(II)-PLSC

Cu(II)-PLSC was prepared by the by the addition of 0.1636 g (1 mmol)  $\text{CuCl}_2 \cdot 2\text{H}_2\text{O}$  (in 10 ml distilled water) to a hot aqueous solution 0.5 g (2 mmol) of the Schiff base ligand (in 40 ml distilled water) and refluxed for two hr. A green colored precipitate was formed on adjusting the pH to 7 using a mixture of methanol and ammonia solution. The mixture was continued to reflux for another hr. Then the precipitate was filtered, washed several times with hot distilled water, finally with petroleum ether and air dried.

#### [Cu(HL $\cdot$ ) $_2$ ].H $_2$ O

(Yield: 0.34 g, 71%). IR:  $\nu_{\text{max}}/\text{cm}^{-1}$ : 3466 s, 3377 m, 2899 m, 1585 m, 1545 m, 1500 m, 1263 m, 1132 m, 515-570 m (Cu-O), 430-440 m (Cu-N). ESI-MS in MeOH: m/z 528 [ $\text{M}^+\text{H}$ ]. Elemental analysis: Found (calc.) for  $\text{C}_{18}\text{H}_{24}\text{CuN}_8\text{O}_7$ : C, 40.92 (40.90); H, 4.51 (4.54); N, 21.18 (21.21) %.  $\mu_{\text{eff}}=1.6961$  B.M.  $\Lambda_{\text{M}}[\Omega^{-1}\text{cm}^2\text{M}^{-1}, 10^{-3}, \text{DMSO}]$ : 010

### RESULTS AND DISCUSSION

#### Characterization of metal complexes

Both the metal complexes synthesized were colored, amorphous, and stable to air, soluble only in DMSO and DMF. Both the complexes show a very low conductivity indicating non-electrolytic nature of the complexes.

#### Mass spectra

The electrospray ionization mass spectrometry (ESI-MS) studies confirmed the proposed molecular formulae of the metal complexes. [Ni(HL $\cdot$ ).Cl.2H $_2$ O] shows a peak at m/z 355 ( $\text{M}^+\text{H}$ ), and [Cu(HL $\cdot$ ) $_2$ ].H $_2$ O at m/z 528 ( $\text{M}^+\text{H}$ ) indicating the stoichiometric ratios 1:1 (ML) for [Ni(HL $\cdot$ ).Cl.2H $_2$ O] and 1:2 (ML $_2$ ) for [Cu(HL $\cdot$ ) $_2$ ].H $_2$ O complexes respectively (Figures 1 and 2).

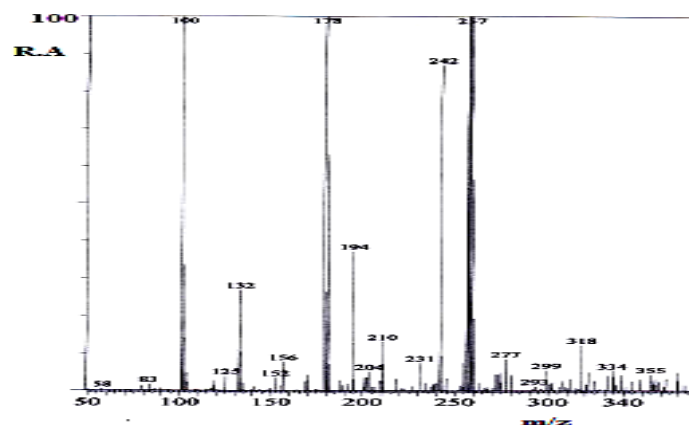


Figure 1: ESI-mass spectrum of [Ni(HL $\cdot$ ).Cl.2H $_2$ O]

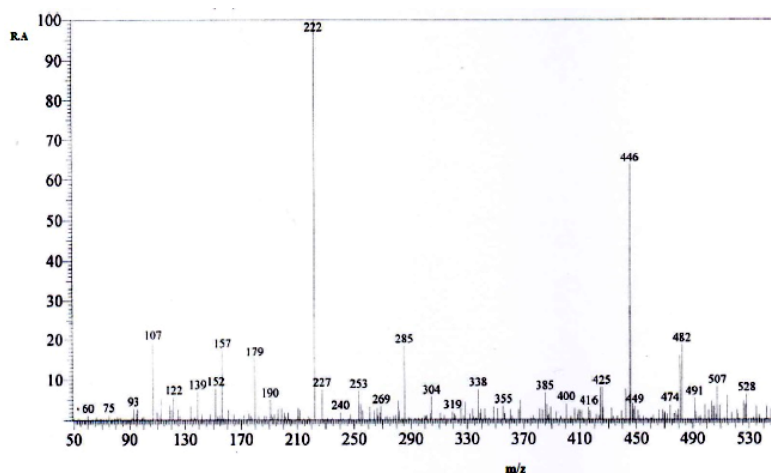


Figure 2: ESI-mass spectrum of  $[\text{Cu}(\text{HL}^-)_2]\cdot\text{H}_2\text{O}$

#### IR spectral analysis

Comparison of the spectra of the complexes with that of ligands indicates the formation of complexes by coordination through ONO atoms (phenolic oxygen, azomethine nitrogen and amide oxygen) in PLSC. The IR data suggests the involvement of mono-anionic form of ligands in both the complexes, where the band for hydrazine  $-\text{NH}$  is missing in the complexes due to the loss of proton of this group. Bands in the region  $3000\text{--}3500\text{ cm}^{-1}$  in the ligands and complexes are attributed to  $\nu(\text{N-H})$  of amino group and  $\nu(\text{O-H})$  vibrations of the  $\text{CH}_2\text{OH}$  group and phenolic hydroxyl group. A medium band at  $3136\text{ cm}^{-1}$  indicative of hydrazine  $-\text{NH}$  in the ligand has disappeared in the complexes suggesting loss of proton on this group and formation of mono anionic form of ligand. A medium band in the range  $2800\text{--}2900\text{ cm}^{-1}$  assigned for  $\nu(\text{NH}^+)$  of the pyridine ring, which is formed as a consequence of shifting of proton from the phenolic group to the pyridine nitrogen, is retained in the complexes. A new band has appeared in the complexes in the region  $1550\text{--}1600\text{ cm}^{-1}$  indicating the formation of new  $\text{C}=\text{N}$  due to enolization of carbonyl group during complexation. A very intense band at  $1703\text{ cm}^{-1}$  assigned for amide  $-\text{C}=\text{O}$  stretch in PLSC has disappeared in its complexes indicating coordination of the ligand to the metal ion through oxygen atom of the carbonyl group. The frequencies of azomethine group in both the complexes have been shifted compared to ligands in the range of  $1550\text{--}1600\text{ cm}^{-1}$  suggesting coordination of nitrogen atom of this group to the metal ion. Shifting in the frequency of the  $\text{Py-C-O}$  vibration in the range  $1100\text{--}1200\text{ cm}^{-1}$  indicates the involvement of phenolic oxygen in coordination (Figures 3 and 4).

#### Thermal analysis

Thermo gram of  $[\text{Ni}(\text{HL}^-)\cdot\text{Cl}\cdot 2\text{H}_2\text{O}]$  shows weight loss (10%) between  $170\text{--}280^\circ\text{C}$ , with an endothermic peak in DTA curve between  $160\text{--}240^\circ\text{C}$ , indicating the loss of two coordinated water molecules.  $[\text{Cu}(\text{HL}^-)_2]\cdot\text{H}_2\text{O}$  shows a weight loss (4%) between  $140\text{--}150^\circ\text{C}$ , with an endothermic peak in DTA curve at  $140^\circ\text{C}$ , which corresponds to dehydration of one lattice water molecule. Both the complexes show a similar behavior after  $300^\circ\text{C}$  in TGA with a loss in ligand moiety accompanied by an exothermic peak in DTA suggesting a rearrangement in the structure of these complexes at this temperature (Figures 5 and 6) [26].

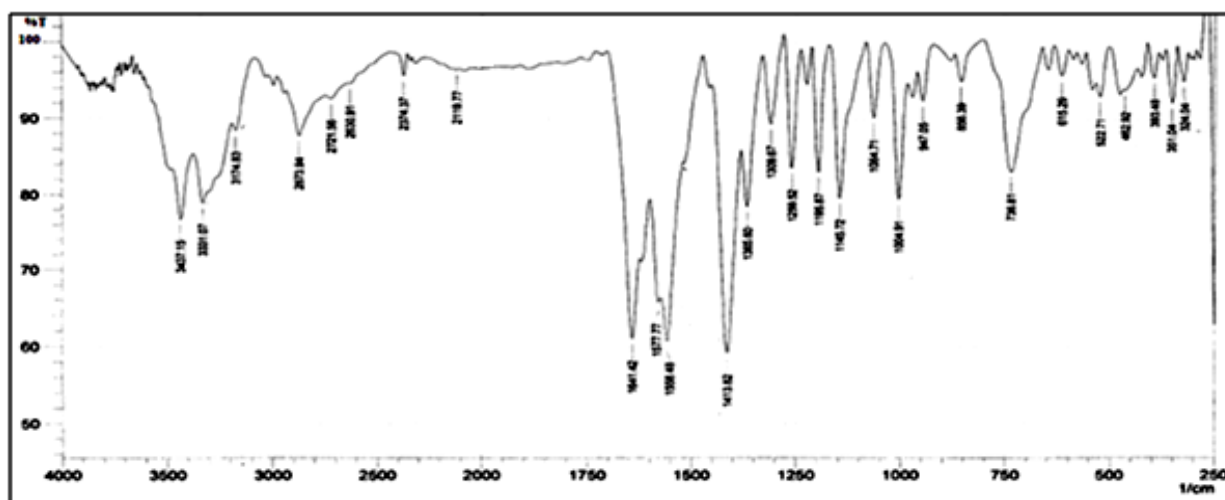
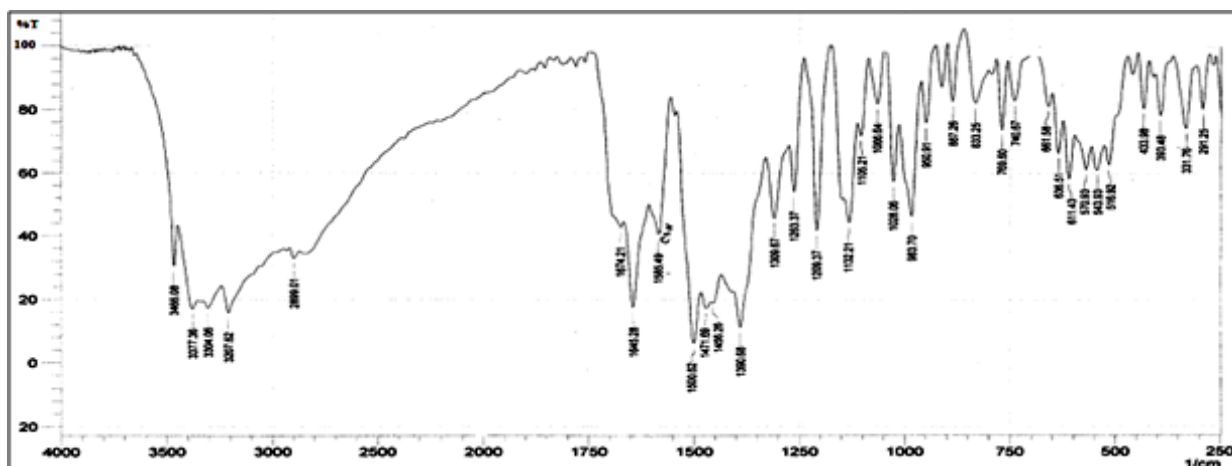
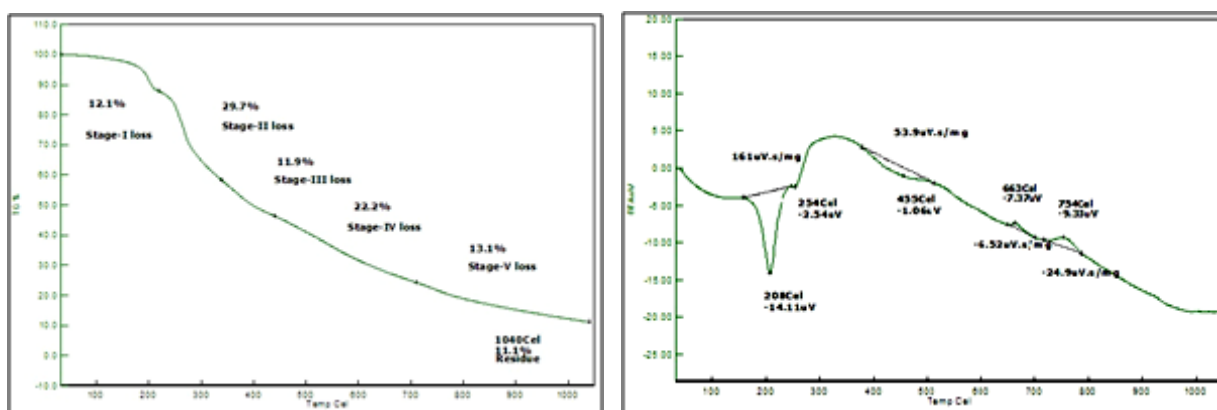
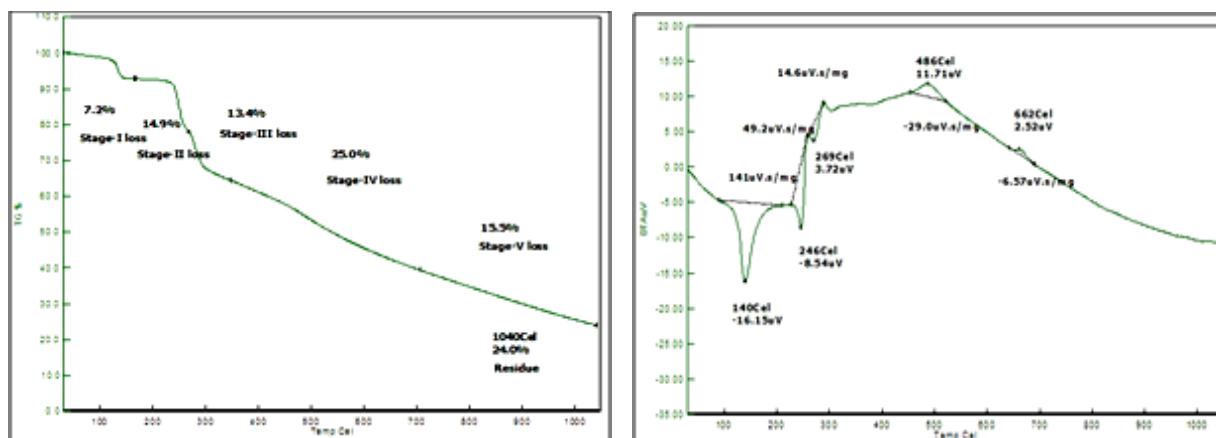


Figure 3: IR spectrum of  $[\text{Ni}(\text{HL}^-)\cdot\text{Cl}\cdot 2\text{H}_2\text{O}]$

Figure 4: IR spectrum of  $[Cu(HL-2)] \cdot H_2O$ Figure 5: TGA and DTA curves of  $[Ni(HL-).Cl.2H_2O]$ Figure 6: TGA and DTA curves of  $[Cu(HL-2)] \cdot H_2O$ 

#### UV-visible spectra

The electronic absorption spectra of the ligand and its metal complexes were recorded in DMSO solution at room temperature. The UV-Vis spectrum of PLSC shows a band at  $33,422 \text{ cm}^{-1}$  (with a shoulder at  $29,904 \text{ cm}^{-1}$ ), which is assigned to the  $n-\pi^*$  transition of the  $C=N$  chromophore. On complexation, this band is shifted to lower wavelength in the complexes, indicating coordination of azomethine nitrogen to the metal ion.

The number and position of d-d transitions in the electronic spectrum of a metal complex gives valuable information about the geometry of the complex. Three d-d transitions are observed in the electronic spectrum of  $[Ni(HL-).Cl.2H_2O]$  at  $11,286 \text{ cm}^{-1}$ ,  $14,492 \text{ cm}^{-1}$  and  $25,075 \text{ cm}^{-1}$  due to  ${}^3A_{2g} \rightarrow {}^3T_{2g}$ ,  ${}^3A_{2g} \rightarrow {}^3T_{1g}$  (F) and  ${}^3A_{2g} \rightarrow {}^3T_{1g}$  (P) respectively indicating an octahedral geometry for this complex. Similarly, three d-d transitions are also observed in the electronic spectrum of  $[Cu(HL-2)] \cdot H_2O$  at  $10,787 \text{ cm}^{-1}$ ,  $16,168 \text{ cm}^{-1}$  and  $24,937 \text{ cm}^{-1}$  due to  ${}^2B_{1g} \rightarrow {}^2A_{1g}$ ,  ${}^2B_{1g} \rightarrow {}^2B_{2g}$  and  ${}^2B_{1g} \rightarrow {}^2E_{1g}$  respectively indicating a distorted octahedral geometry for this complex (Figure 7) [27].

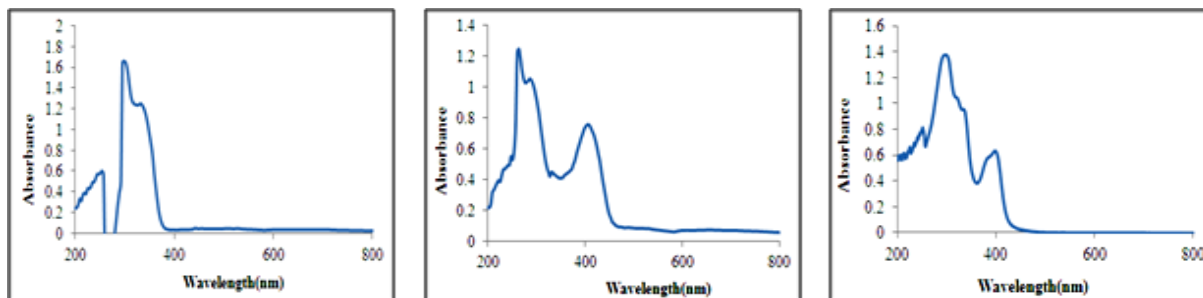


Figure 7: Electronic spectra of PLSC, [Ni(HL).Cl.2H<sub>2</sub>O] and [Cu(HL)<sub>2</sub>].H<sub>2</sub>O

#### Magnetic moments

The magnetic moment values  $\mu_{\text{eff}}$  of [Ni(HL).Cl.2H<sub>2</sub>O] is found to be 2.8835 BM indicating the presence of two unpaired electrons in the central metal ion. Whereas the magnetic moment of [Cu(HL)<sub>2</sub>].H<sub>2</sub>O is found to be 1.6961 BM indicating the presence of single unpaired electron. Magnetic moment values of these complexes also suggest their paramagnetic nature.

Based on the spectral and analytical data the structures of the Ni(II) and Cu(II) complexes of PLSC are proposed as shown in Figures 8a and 8b.

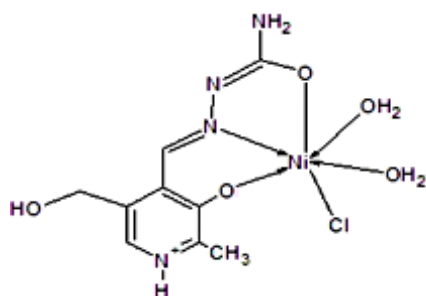


Figure 8a: Structure of [Ni(HL).Cl.2H<sub>2</sub>O]

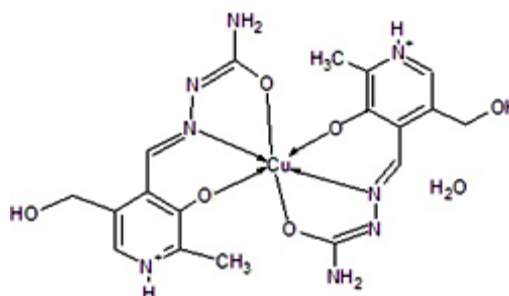


Figure 8b: Structure of [Cu(HL)<sub>2</sub>].H<sub>2</sub>O

#### DNA binding experiments

##### Absorption spectral titration

UV-Vis absorption spectroscopy is the most commonly used method to assess the interaction of DNA with the metal complexes. This technique involves monitoring the changes in the UV-Vis spectrum of a complex during its interaction with DNA. It is determined by examining the modifications in the  $\lambda_{\text{max}}$  values of  $\pi-\pi^*$  intra ligand transitions, or LMCT or d-d transitions of a metal complex with the increase in the concentration of DNA [28]. An intercalative mode of binding of a metal complex to DNA is indicated by hypochromism and bathochromism or hypsochromism, while hyperchromism suggests electrostatic interaction or groove binding. The extent of changes in the absorption of the metal complex spectrum is consistent with the strength of interaction [29].

In the present study, both the metal complexes [Ni(HL).Cl.2H<sub>2</sub>O] and [Cu(HL)<sub>2</sub>].H<sub>2</sub>O show hypochromism and bathochromism with the increase in concentration of DNA indicating the binding of the complexes through intercalation, which involves the insertion of the planar aromatic chromophore of the ligand in between the base pairs of DNA. The extent of hypochromism is consistent with the strength of intercalative interaction. The DNA binding affinities of the complexes is quantitatively expressed in terms of intrinsic binding constant ( $K_b$ ) which is found to follow the order [Cu(HL)<sub>2</sub>].H<sub>2</sub>O > [Ni(HL).Cl.2H<sub>2</sub>O].  $K_b$  values were determined using equation 1 and found to be  $4.0 \times 10^4$  and  $1.0 \times 10^5$  of the complexes [Ni(HL).Cl.2H<sub>2</sub>O] and [Cu(HL)<sub>2</sub>].H<sub>2</sub>O respectively (Figure 9).

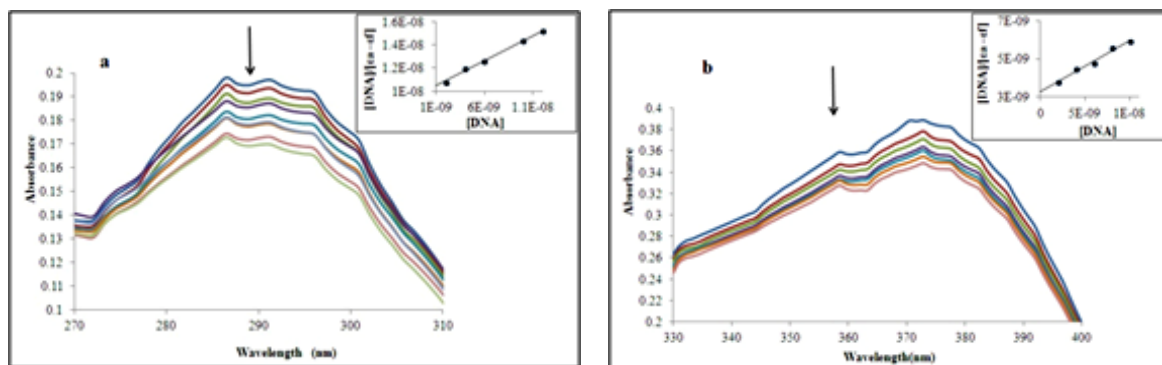


Figure 9: Absorption spectra of the complexes [Ni(HL).Cl.2H<sub>2</sub>O] and [Cu(HL)<sub>2</sub>].H<sub>2</sub>O (20  $\mu\text{M}$ ) in phosphate (pH 7.2) buffer upon addition of CT-DNA (0-20  $\mu\text{M}$ ). Arrow indicates hypochromism with increase in concentration of DNA. Inset: Plot of [DNA]/( $\epsilon b - \epsilon f$ ) versus [DNA] for absorption titration of CT DNA with the complex

## Competitive DNA binding studies of the complexes and ethidium bromide

Ethidium Bromide (EB) strongly interacts with the DNA double helix, by its insertion between the adjacent base pairs and is a well-known classical intercalator. It shows high fluorescence when bound to nucleic acid and hence widely used as a sensitive fluorescent probe for DNA. In buffer solution, the free EB shows decreased emission intensity as a result of the solvent quenching. But it shows a remarkable increase in fluorescence when bound to DNA, as the nucleobases provide a steric protection to the dye molecule [30]. The presence of another species which has affinity towards DNA results in a reduced emission intensity of the EB-DNA adduct, which is caused by a competition for the binding site. The affinity of transition metal complexes towards DNA can be evaluated by competitive fluorescence studies, as it measures the extent of the reduction in emission intensity of the EB-DNA adduct [31].

When the complexes  $[\text{Ni}(\text{HL}^-)\cdot\text{Cl}\cdot 2\text{H}_2\text{O}]$  and  $[\text{Cu}(\text{HL}^-)_2]\cdot\text{H}_2\text{O}$  were added to DNA pretreated with EB, the DNA induced emission intensity of EB was decreased. As the complexes have planar ligand, they replace EB from intercalative binding sites due to which quenching of emission intensity of DNA-bound EB is observed [19]. The quenching plots of  $I_0/I$  versus  $[\text{Complex}]/[\text{DNA}]$  (insets of Figure 10) are in good agreement with the linear Stern-Volmer equation. Stern-Volmer quenching constants ( $K_{sv}$ ) were calculated as 0.1071 and 0.1238 respectively for the complexes  $[\text{Ni}(\text{HL}^-)\cdot\text{Cl}\cdot 2\text{H}_2\text{O}]$  and  $[\text{Cu}(\text{HL}^-)_2]\cdot\text{H}_2\text{O}$ .

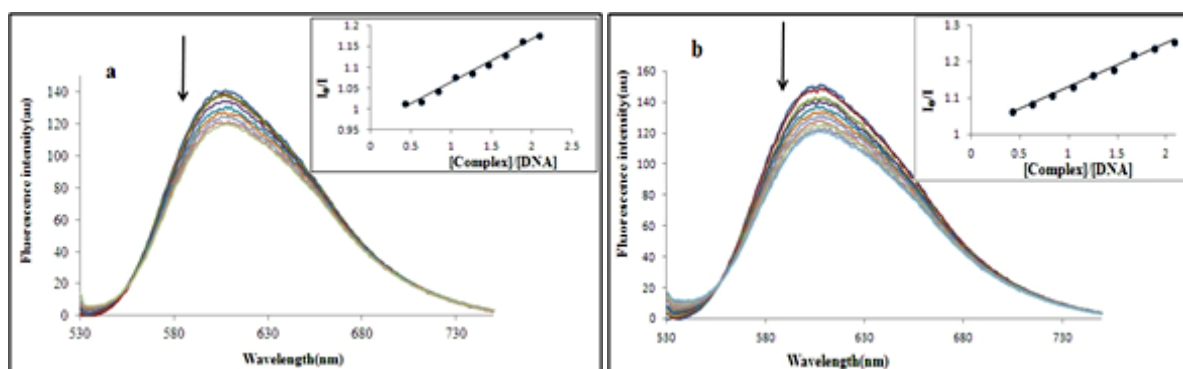


Figure 10: Emission spectra of EB bound CT DNA in the absence and presence of complexes. Arrow shows the decrease in the emission intensity with the increase in complex concentration. Inset: Plot of  $I_0/I$  versus  $[\text{Complex}]/[\text{DNA}]$

## Viscometric measurements

The binding mode of the metal complexes with DNA was further evaluated by viscometric measurements. Although spectroscopic methods provide important evidence to support the mode of binding of metal complexes to DNA, hydrodynamic measurements are considered to be least ambiguous and critical test of a DNA binding model in solution, in the absence of crystallographic data. Intercalation of metal complex leads to lengthening of DNA helix, due to the separation of base pairs to accommodate the binding ligand which further leads to an increase in DNA viscosity. Whereas a bend or kink in the DNA helix may be resulted by partial or non-classical intercalation of ligand, which leads to a decrease in the length of DNA helix and subsequently viscosity [32].

The effect of EB and the metal complexes of PLSC on the viscosity of DNA were studied to understand the binding mode of complexes with the DNA. Figure 11 shows the changes in the viscosity of DNA in the presence of EB and complexes. EB being a potential intercalator shows a significant increase in the viscosity, while the complexes showed the same effect to a less extent indicating insertion of the ligands in between the base pairs of DNA.

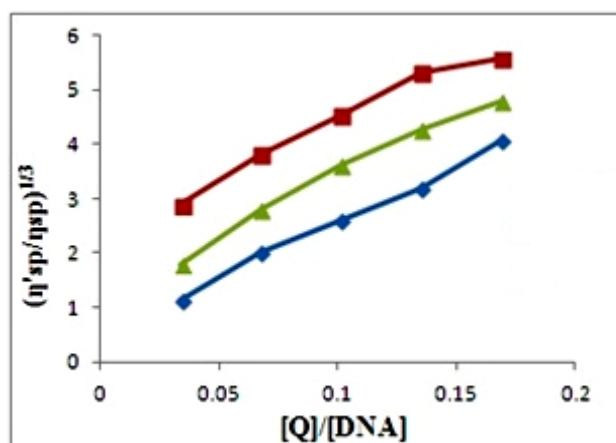


Figure 11: Effect of increasing amounts of the (■) EB, (●)  $[\text{Ni}(\text{HL}^-)\cdot\text{Cl}\cdot 2\text{H}_2\text{O}]$  and (▲)  $[\text{Cu}(\text{HL}^-)_2]\cdot\text{H}_2\text{O}$  on the relative viscosities of CT DNA at 25°C

### DNA cleavage without added reagents

Purines and pyrimidines act as building blocks in nucleic acids which are joined by phosphodiester linkages. Phosphodiester bond in DNA is highly inert towards hydrolysis under physiological conditions due to its high half-life period of the order of billions of years. The negative charge of the phosphodiester bond disfavors its hydrolysis through nucleophilic attack. Therefore for the same reaction to be facilitated, presence of a Lewis acid like a metal ion is required. Metal ions activate the nucleophilic attack by water or hydroxide on phosphate group and enhance the leaving group ability of alcohol [33].

Metal ion mediated hydrolysis of nucleic acids can be exploited in the design of artificial restriction endonucleases. Hydrolytic cleavage of nucleic acids is preferable over redox-mediated cleavage reactions, as the information during the hydrolytic reaction is preserved. The fragments thus produced are useful in gene manipulation and in understanding the roles of metal ions in metalloenzyme catalysis [33].

DNA cleavage ability of the complexes was evaluated using super coiled (SC) plasmid pBR322 DNA (100 ng/ $\mu$ L). The DNA was incubated with varying concentrations of complexes (20-60  $\mu$ M in DMSO), in Tris-HCl buffer (pH 7.2) for 1 hr at 37°C. It was observed that both the complexes are able to cleave DNA without any added reagents or light as they contain nucleophiles such as coordinated water molecules and/or hydroxyl groups in the ligands, indicating the hydrolytic cleavage of DNA. Figure 12 depicts the cleavage of super coiled DNA by the complexes with partial degradation of SC form to produce NC form at a very low concentration as 20-60  $\mu$ M.

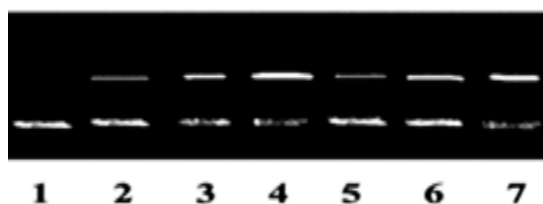


**Figure 12:** Agarose gel electrophoresis pattern for the cleavage of supercoiled pBR 322 DNA by complexes. Lane 1, DNA control, Lane 2-4 DNA+[Ni(HL).Cl.2H<sub>2</sub>O] (20  $\mu$ M, 40  $\mu$ M, 60  $\mu$ M respectively), Lane 5-7 DNA+[Cu(HL)<sub>2</sub>].H<sub>2</sub>O (20  $\mu$ M, 40  $\mu$ M, 60  $\mu$ M respectively)

### Antibacterial activity

The complexes could not inhibit the growth of gram negative bacteria while they showed moderate activity towards gram positive bacteria which was indicated by the zone of inhibition. [Ni(HL).Cl.2H<sub>2</sub>O] showed a zone of inhibition of 12 mm and 9 mm, while [Cu(HL)<sub>2</sub>].H<sub>2</sub>O showed 15 mm and 11 mm against *Staphylococcus aureus* and *Bacillus subtilis* respectively.

### CONCLUSION

Pyridoxal semicarbazone forms complexes with Ni(II) and Cu(II) ions by coordination through ONO atoms. [Ni(HL).Cl.2H<sub>2</sub>O] is formed in 1:1(ML) while [Cu(HL)<sub>2</sub>].H<sub>2</sub>O, is formed in 1:2 (ML<sub>2</sub>) ratios. Both the complexes exhibited octahedral geometry. The complexes were evaluated for their DNA binding activity by absorption titrations, fluorescence spectra and viscometric measurements which suggest that both the complexes are able to bind DNA effectively even at very low concentrations through intercalation. The complexes also exhibited plasmid DNA cleavage ability by hydrolytic pathway. The complexes showed a moderate antibacterial activity against gram positive bacteria.

### ACKNOWLEDGEMENTS

The authors are thankful to University Grants Commission, New Delhi for financial support and also Osmania University, Hyderabad and St. Francis College for Women, Hyderabad for providing necessary facilities to carry out this work.

### REFERENCES

- [1] S. Padhye, G.B. Kauffman, *Coord. Chem. Rev.*, **1985**, 63, 127-160.
- [2] H. Chen, X. Ma, Y. Lv, L. Jia, J. Xu, Y. Wang, Z. Ge, *J. Mol. Struct.*, **2016**, 1109, 146-153.
- [3] Y. Li, Z. Yang, Z. Liao, Z. Han, Z. Liu, *Inorg. Chem. Comm.*, **2010**, 13(10), 1213-1216.
- [4] Z. Afrasiabi, E. Sinn, W. Lin, Y. Ma, C. Campana, S. Padhye, *J. Inorg. Biochem.*, **2005**, 99(7), 1526-1531.
- [5] S. Chandra, L.K. Gupta, *Spectrochem. Acta. Part A: Mol. Biomol. Spectro.*, **2005**, 62 (4-5), 1089-1094.
- [6] U. Kumar, S. Chandra, *J. Saudi. Chem. Soc.*, **2011**, 15 (2), 187-193.
- [7] S. Goel, S. Chandra, S.D. Dwivedi, *J. Saudi. Chem. Soc.*, **2013**.
- [8] N.Z. Knezevic, V.M. Leovac, V.S. Jevtovic, S.G. Sipka, T.J. Sabo, *Inorg. Chem. Comm.*, **2013**, 561-564.
- [9] D. Vidovic, A. Radulovic, V. Jevtovic, *Polyhedron.*, **2011**, 30 (1), 16-21.
- [10] V.M. Leovac, V.S. Jevtovic, L.S. Jovanovic, G.A. Bogdanovic, *J. Serb. Chem. Soc.*, **2005**, 70(3), 393-422.



- [11] V.M. Leovac, L.S. Jovanovic, V. Divjakovic, A. Pevec, I. Leban, T. Armbruster, *Polyhedron.*, **2007**, 26, 49-58.
- [12] V. Jevtovic, D. Cvetkovic, D. Vidovic, *J. Iran. Chem. Soc.*, **2011**, 8(3), 727-733.
- [13] V. Jevtovic, *Res. Cancer. Tumor.*, **2014**, 3(1), 1-5.
- [14] V.S. Jevtovic, G. Pelosi, S. Ianeli, R. Kovacevic, S.N. Kaisarevic, *Acta. Chim. Slov.*, **2010**, 57, 363-369.
- [15] P. Kavitha, M.R. Chary, B.V.V.A. Singavarapu, K.L. Reddy, *J. Saudi. Chem. Soc.*, **2016**, 20(1), 69-80.
- [16] N. Shahabadi, S. Kashanian, F.Darabi, *Europ. J. Med. Chem.*, **2010**, 45(9), 4239-4245.
- [17] N. Raman, S. Sobha, L. Mitu, *J. Saudi Chem. Soc.*, **2013**, 17(2), 151-159.
- [18] A.N.M.A. Alaghaz, M.E. Zayed, S.A. Alharbi, *J. Mol. Struc.*, **2015**, 182, 62-79.
- [19] E.W.Y. Tido, C. Faulmann, R. Roswanda, A.Meetsma, P.J. Van Koningsbruggen., *Dalton Trans.*, **2010**, 39, 1643-1651.
- [20] B.N. Figgis, J. Lewis, In: J. Lewis, R.C. Wilkins, Ed., NY, USA, *Mod. Coord. Chem.*, **1960**.
- [21] S.S. Bhat, A.A. Kumbhar, H. Heptullah, A.A. Khan, V.V. Gobre, S.P. Gejji, V.G. Puranik, *Inorg. Chem.*, **2011**, 50, 545-558.
- [22] A.K. Srivastava, N. Kumari, R.A. Khan, R. Rai, G. Rai, S. Tabassum, L. Mishra. *Ind. J. Chem.*, **2013**, 52A, 835-844.
- [23] S.S. Bhat, A.S. Kumbhar, P. Lonneck, E.H. Hawkins, *Inorg. Chem.*, **2010**, 49, 4843-4853.
- [24] B. Biswas, M. Mitra, A. Pal, A. Basu, S. Rajalakshmi, P. Mitra, N.A. Alkalde, G.S. Kumar, B.U. Nair, R. Ghosh, *Ind. J. Chem.*, **2013**, 52A, 1576-1583.
- [25] M. Balouiri, M. Sadiki, S.K. Ibnsouda, *J. Pharm. Anal.*, **2016**, 6(2), 71-79.
- [26] V.M. Leovac, S. Markovic, V. Divjakovic, K.M. Szecsenyi, M.D. Joksovic, I.Leban, *Acta. Chim. Slov.*, **2008**, 55, 850-860.
- [27] A.B.P. Lever, 2<sup>nd</sup> Edn., Elsevier Publishing Co., Amsterdam, **1984**.
- [28] N. Raman, S. Sobha, *Spectrochim. Acta. A. Mol. Biomol. Spectrosc.*, **2012**, 85(1),223-34.
- [29] M. Ashfaq, T. Najam, S.S. Shah, M.M. Ahmad, S. Shaheen, R. Tabassum, G. Rivera, *Curr. Med. Chem.*, **2014**, 21(26), 3081-3094.
- [30] T. Topala, A. Bodoki, L. Oprean, R. Oprean, *Formacia*, **2014**, 62(6), 1049-1061.
- [31] L. Jin, P. Yang, *Polyhedron*, **1997**, 16(19), 3396-3398.
- [32] P. Nagababu, M. Shilpa, J.N.L. Latha, I. Bhatnagar, P.N.B.S. Srinivas, Y.P. Kumar, K.L. Reddy, S. Satyanarayana, *J. Fluores.*, **2011**, 21(2), 563-572.
- [33] P.R. Reddy, A. Shilpa, *Chem. Biodivers.*, **2011**, 8, 1245.